AJDS LAZHAR Al-Azhar Journal of Dental Science
Vol. 28- No. 1- 61:70- January 2025
Print ISSN 1110-6751 | online ISSN 2682 - 3314
https://ajdsm.journals.ekb.eg
Oral Biology, Medicine & Surgical Sciences Issue *(Oral Biology, Oral Pathology, Oral Periodontology, Medicine, Oral & Maxillofacial Surgery)*

THE EXPRESSION PATTERN OF BMI 1 CAN PREDICT THE THERAPEUTIC POTENTIAL OF PIPERINE IN EXPERIMENTALLY INDUCED HAMSTER BUCCAL POUCH CARCINOMA (HISTOLOGICAL AND IMMUNOHISTOCHEMICAL STUDIES)

Hassan Ali Mohamed[1*], Amr Mohamed Ibrahim [2,3], Ahmed Elshafei [4],
Mohamed Mahmoud Ahmed Ahmed [5]

ABSTRACT

Objective: One of the goals of the study was to investigate the expression pattern of Bmi1 of treated hamsters with piperine after experimentally induced HBP carcinoma. **Subjects and methods:** Thirty male Syrian hamsters were randomly split into three groups (G(s)) of ten. Hamsters in groups II and III had 7, 12-dimethylbenz (a) anthracene (DMBA) painted into their right hamster buccal pouch (HBP) three times a week for 14 weeks, whereas hamsters in group I (control) were left untreated for 22 weeks. After that, the animals in GII (positive control) were left with no additional treatment for other 8 ws (total period 22 ws), whereas those in GIII were treated by piperine (50 mg/kg, orally) daily for 4ws, and then, animals were left with no additional treatment for other 4 ws (total period 22 ws). After termination of the experiment, After euthanizing the animals, HBP were surgically removed, cleaned, fixed, and processed for a histological analysis and categorization using H&E stain, and immunohistochemical (IHC) staining utilizing Bmi1 cancer stem cell(CSC) antibody. **Results:** The gap between GII and GIII was statistically very significant (p value < 0.001) regarding to tumor volume, depth of invasion(DOI) and regarding nuclear expression of Bmi1which revealed that, GI had the smallest average surface area (9.71%), whereas GII had the largest average surface area (65.88%), followed by GIII **Conclusions:** Piperine could inhibit HBP squamous cell carcinoma (SCC) in addition to, downregulation of Bmi1 can predict the therapeutic potential of piperine in HBP SCC.

KEYWORDS: HBP carcinoma, piperine, Bmi1.

1. Assistant Lecturer, Oral and Dental Pathology Department, Faculty of Dental Medicine (Boys- Cairo), Al-Azhar University, Egypt.
2. Assistant Professor, Oral and Dental Pathology Department, Faculty of Dental Medicine (Boys- Cairo), Al-Azhar University, Egypt.
3. Assistant Professor, Head of Basic Dental Sciences Department, Faculty of Dentistry, Deraya University, New Minia, Minia, Egypt.
4. Professor Associate, Department of Biochemistry and Molecular Biology, Faculty of Pharmacy, (Boys-Cairo), Al-Azhar University, Egypt.
5. Professor, Oral and Dental Pathology Department, Faculty of Dental Medicine (Boys-Cairo), Al-Azhar University, Egypt.

• ***Corresponding author*:** hassanomarwan@gmail .com

DOI: *10.21608/ajdsm.2023.221923.1439*

INTRODUCTION

In Egypt, oral cancer ranged from 3.546% to 9.6639% of total number of reported malignancies from 2016 to 2021 Although oral squamous cell carcinoma (OSCC) is the most common malignancy of the oral region with 59.49 % [1]. OSCC refer to any malignant development in the mouth, lips, tongue, or throat is called oral cancer. Lip, cheek, gum, floor of mouth, soft and hard palate, sinuses, tonsils, salivary glands, and throat tumors are all part of this deadly malignancy[2]. Premalignant dysplastic lesions, such as erythroplakia, leukoplakia, lichen planus, or a combination of these disorders may lead to the development of oral squamous cell carcinoma (OSCC [3]. Exposure to well-known carcinogens including alcohol, cigarettes, betel nut, and human papillomavirus (HPV) infection, especially in the presence of premalignant lesions, may increase the risk of OSCC development. Once OSCC have formed, tumor cells may extensively infiltrate neighboring tissues and lymph nodes in the neck, eventually spreading to other parts of the body [4,5]. Histological classification of OSCC often includes well-differentiated cells that closely resemble normal surface epithelium and nests of tumor cells that destroy the basement membrane. Disorganized development, dyskeratosis, loss of polarity, keratin pearls, a high nuclear-to-cytoplasmic ratio, and increased mitotic figures (including atypical forms) are all hallmarks of OSCC [6]. Mitotic features and necrosis are more common in poorly differentiated OSCC correlate positively with metastatic potential[6]. It has shown that DMBA is an effective site specific carcinogenic agent for inducing oral carcinogenesis[7]. There has been progress in OSCC diagnosis and treatment approaches in recent years, but the 5-year survival rate is still rather low[8]. Eighty percent of all synthetic medications are derived from natural medicinal plants[9]. These plant-based active chemicals have been shown to considerably enhance the treatment of cancer[10]. In this light, numerous natural compounds, including piperine, have been studied for their potential anticancer effects. Piperine's anti-cancer activities are based on its ability to regulate multiple signaling molecules, including those involved in preventing cell growth[11], stopping the cell cycle[12], causing DNA damage in tumor cells, triggering apoptosis, and shifting redox balance[13] Self-renewing and asymmetrically dividing cells are what give CSCs their name, which is considered the main cause of cancer cell development, metastasis, and tumor recurrence after therapy. Recent research shows that CSC targeting as a therapy approach for cancer has showed promise [14,15]. CSC indicators that may be beneficial in therapeutic, diagnostic, and prognostic methods are highlighted, with special attention paid to the most lethal of malignancies, OSCC[16].

High levels of Bmi1 expression in cancer were associated with EMT and a dismal outcome. Bmi1 expression is commonly uncontrolled in a wide range of human malignancies, according to a large body of research [17, 18].

Thus, the primary purpose of this investigation was to evaluate piperine's effect on DMBA-induced HBP cancer. The evaluation relied on the HBP gross findings, the histological alterations in the tumor tissue, and the IHC expression of Bmi1.

SUBJECTS AND METHODS

Chemicals

DMBA (0.5 percent - Sigma-Aldrich) was dissolved by adding 0.5 gm into 100 ml of paraffin oil. Corn oil was used to dissolve piperine (Sigma-Aldrich Corporation in Steniheim, Germany).

Animals

Five-week-old male Syrian hamsters weighing 80-120g were purchased from a private animal house in Cairo.

Sample size

Based on, Gkoulioni, et al [19] research and Annie W et al, [20] reported that, a sample size of 10 in each group, in the current study, will have 85% power

to detect a difference between means of 0.53 with a significance level (alpha) of 0.05 (two-tailed) at 95% confidence intervals. In 85% (the power) of those experiments, the p value will be less than 0.05 (two-tailed) so the results will be deemed "statistically significant". In the remaining 15% of the experiments, the difference between means will be deemed "not statistically significant". Report created by GraphPad StatMate 2.00.

Experimental design

After a week of adjustment, the animals were randomly split into three distinct sets of ten. HBP in groups GII and GIII were painted with 0.5 percent DMBA in liquid paraffin with a number 4 camel hair brush three times a week for fourteen weeks, whereas animals in group GI were left untreated. The animals in Group II (the positive control) had no further treatment for another 8 weeks, whereas those in Group III (the experimental group) were given piperine (50 mg/kg, orally) daily for 4 weeks, and then received no further treatment for another 4 weeks .

Tumor volume measurement

Following the completion of the trial, the right HBP was everted, the animals were euthanized by inhalation of di- ethyl ether, and the tumor diameters were measured using a Vernier caliper. Vmm3 = (4/3) [(D1/2) (D2/2) (D3/2)], where D1, D2, and D3 are the tumor's three diameters (mm), and is the ratio of the circumference to the diameter of a circle, which is roughly equal to 3.14159.

Histopathological examinations

Tissue samples were sectioned, fixed in a 10% formalin solution, washed in an escalating ethanol series, and finally inserted into paraffin wax blocks. For histological analysis, 4-micrometer-thick tissue slices were cut using a rotary microtome, mounted on glass slides, handled, and stained with H&E.

Measurement of the depth of invasion (DOI)

All surgical specimens were evaluated for DOI using H&E slides. The depth of the tumor nest was calculated as the distance between the surface epithelium's basement membrane to the tumor's center. The American Joint Committee on Cancer (AJCC) further divides it into three stages based on tumor invasion depth: minimal (≤ 5 mm), moderate (6-10 mm), and severe (≥ 10 mm)(23). DOI was determined using a Leica QWIN V3 image analyzer computer system (Switzerland) run by Leica QWIN V3 software at the oral and dental surgery department of Al-Azhar University's Faculty of Dental Medicine (Boys-Cairo), Egypt.

Immunohistochemical examination

For the standard labeled streptavidin-biotin approach, 3 m tissue slices were placed on positively charged slides to display Bmi1 antibody expression. After being immersed in xylene for five minutes, the sections underwent a Five-minute cycle of graded ethanol (100%, 95%, and 70%) to rehydrate the tissue. The slides were washed for five minutes each in a mixture of distilled water and phosphate buffered saline (PBS). For thirty minutes at ambient temperature, three percent hydrogen peroxide (H2O2) in methanol solution inhibited endogenous peroxidase activity. PBS was then used to clean the slides. The slides were then placed in 200 cc of citrate buffer (pH 6) in plastic jars. The jars were heated at 100 degrees Celsius for 15 minutes at full power, three times. The slides were coaling slowly at room temperature. The slides were then washed twice for 5 minutes, first in distilled water and then in PBS. Primary antibodies against Bmi1 were applied to tissue slices at a dilution of 1:100 and then incubated at room temperature in a humidified chamber overnight. After being rinsed in distilled water, the slides were treated to a 5-minute soak in PBS. The secondary antibody was biotinylated and incubated for 30 minutes at room temperature. After that, the tissue pieces were given a 5-minute wash in PBS. After 30 minutes at room temperature, the cells were washed in PBS and stained with streptavidin

that had been tagged with peroxidase. After being treated with DAB for 2-4 minutes to induce staining, the tissue slices were submerged in distilled water. After being counterstained with Mayer hematoxylin for one minute, tissue slices were rinsed in running water. Before being mounted with DPX and coated with plastic for examination, the slides were given two 3-minute baths in 95% alcohol, followed by two 3-minute baths in pure alcohol. By removing the main antibody, we generated negative controls. Bmi1 was tested against breast cancer samples used as positive controls.

To determine the frequency of positive instances and the precise location of immunostaining within the tissues, a light microscope examination of immunostained sections was performed. Mean area percentage of IHC stainability of cells with Bmi1 antibody was also evaluated using an image analysis computer system. For the purpose of statistical analysis, a mean value was picked from evaluations conducted with a low power lens (1010)).The work was completed at Al-Azhar University in Egypt's Faculty of Dental Medicine (Boys-Cairo).

Statistical analysis

The data was recorded as a mean SD and then examined statistically. Using SPSS 17.0 for Windows, we conducted a one-way analysis of variance (ANOVA). Using ANOVA and the LSD post hoc test, we compared quantitative data from more than two groups with a parametric distribution. If the p value was more than 0.05, it was deemed not significant; if it was less than 0.05, it was regarded significant; and if it was less than 0.001, it was deemed extremely significant.

RESULTS

Gross observation and tumor volume:

Hamsters in each studied group, showed variable results in regard to HBP mucosa gross observation and tumor volume. The right HBP mucosa of all hamsters in **GI** appear normal, pale pink with neither pathological nor inflammatory changes (Fig.1A), also without hair loss or skin ulcers, while **in GII** the right HBP mucosa of all hamsters showed exophytic swellings, 3 hamsters out of 10 showed solitary large exophytic swelling covered by thick whitish membrane, while the others showed multiple exophytic nodules with presence of mucosal ulcers and bleeding areas (Fig. 1B), 2 hamsters out of 10 showed hair loss, and ulcers in skin side of the right HBP, **GIII** the right HBP mucosa of 4 hamsters out of 10 showed multiple small exophytic nodules with presence of thick white patches (Fig.1C), 3 hamsters showed solitary exophytic swelling, while 3 hamsters showed sessile swelling covered by normally appeared mucosa, all hamsters didn't show hair loss, skin and mucosal ulcers.

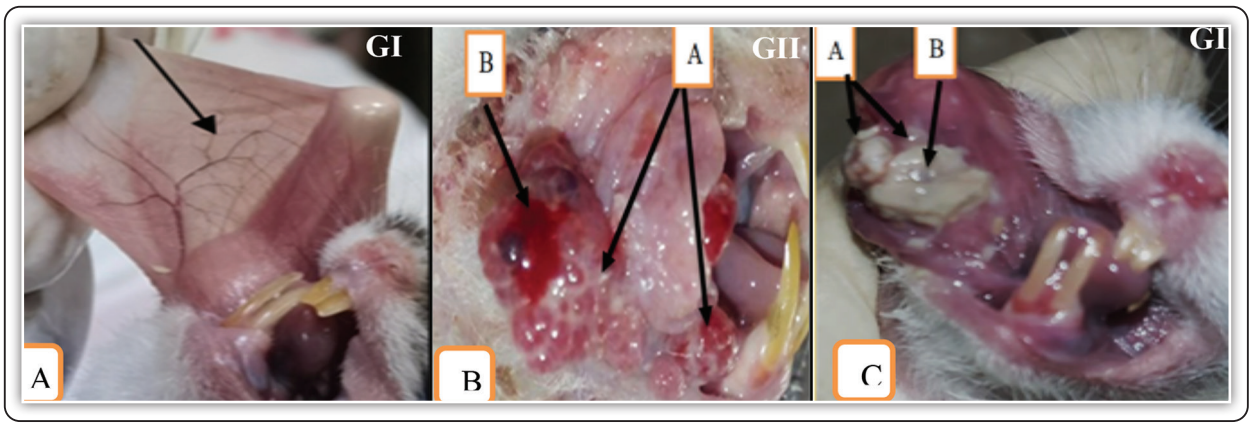

FIG (1) **(A)** Photograph of HBP mucosa of GI pink in color with smooth surface and no observable abnormalities (arrow); **(B)** Photograph of HBP of GII showing multiple exophytic nodules (arrows A) with bleeding area (arrow B); **(C))** Photograph of HBP of GIII showing multiple small exophytic nodules (arrows A) covered by thick white patch (arrow B).

Statistical analysis results of tumor volume:

The mean tumor volume of GIII had recorded the lowest value (395.20 mm^3), while GII had recorded the highest mean tumor volume (770.92 mm^3), there was a high significant difference between GII and GIII (p value < 0.001) Table (1), fig (2).

Histological findings

Histological sections of GI, using H&E stain, exhibited typical mucosal structure, including four layers of squamous cells with little keratinization (i.e., one layer of basal cells, and two or three layers of spinous and thin keratinized cells, devoid of rete ridges). Layers of muscle and connective tissue underneath the epithelium (Fig.3A), while **GII:** revealed that, 7 hamsters out of 10 exhibited well differentiated SCC(Fig.3B) and 3 hamsters exhibited moderately differentiated SCC. The invading epithelial islands into underlying C.T are variable in size, dysplastic features and keratin formation which extend deeply in C.T with mean DOI=10.02mm (Table 2), **GIII** revealed that, 3 hamsters out of 10 showed moderate epithelial dysplasia, 1 hamster showed mild epithelial dysplasia, Carcinoma in situ was found in Two hamsters, whereas SCC with superficial invasion of malignant cells in the form of well-differentiated SCC was seen in 4 hamsters; this SCC was confined to the sub-epithelial area and did not spread to deeper regions of the C.T. (Fig. 3C),with mean DOI= (0 – 2.81) mm (Table 2).

TABLE (1) Comparison between studied groups as regard to tumor volume.

Gs	Tumor volume (mm3)		Post Hoc analysis by LSD		
	Mean ±SD	Range	G I	G II	G III
G I	--	--	--	--	--
GII	770.92 ±138.23	500.72 –951.12	--	--	0.000
GIII	395.20 ±77.56	301.2 –526.56	--	0.000	--
Test value	44.931				
P-value	<0.001 (HS)				

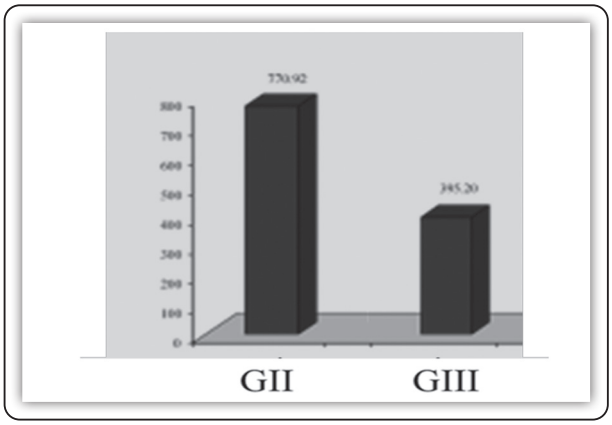

FIG (2) Bar fig representing tumor volume in the studied groups

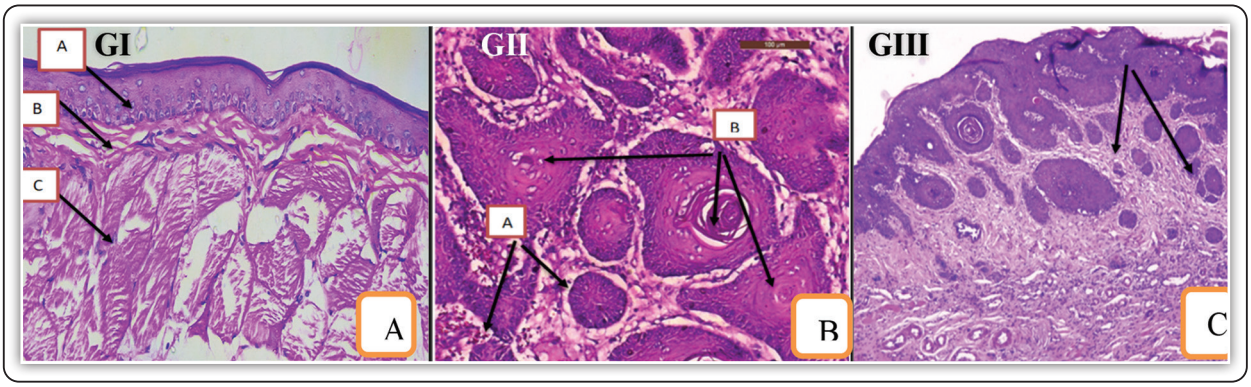

FIG (3) (**A**) H&E stain of GI showing keratinized stratified squamous epithelium (arrow A), sub-epithelial CT layer (arrow B), and muscle layer (arrow C). (X200); **(B)** H&E stain of GII showing well differentiated SCC, with deeply invading multiple epithelial islands into the underlying C.T (arrows A) and keratin pearls (arrows B). (X 200); **(C)** H&E stain of GIII showing well differentiated SCC, with few and small epithelial islands into the underlying CT (arrows). (X 200).

Statistical analysis results of DOI:

There were high significant difference between GII and GIII (p value < 0.001). Table (2), fig (4)

Bmi-1 IHC results:

The IHC staining in GI using Bmi-1 antibody exhibited positive nuclear expression (9.71%) which limited to basal and suprabasal epithelial layer(Table.2)(Fig.5A),while in GII exhibited positive nuclear expression (65.88%)of the invading epithelial islands and negatively stained keratin pearl(Table.2) (Fig.5B),also in GIII Bmi-1 antibody exhibited positive nuclear expression throughout the dysplastic and invading malignant cells (31.09%) (Table.2) (Fig. 5C).

3.6 Statistical analysis results of IHC staining of Bmi-1:

According to the data analysis, GI had the lowest percentage of Bmi1 (9.71%), while GII had the highest percentage (65.88%).There was highly significant between GII and GIII (p=0.001) (Table 3) (fig.6),

TABLE (2) Comparison between studied groups as regard DOI.

	DOI		Post Hoc analysis by Mann Whitney test		
	Median (IQR)	**Range**	**GI**	**GII**	**GIII**
GI	--	--	--	--	--
GII	10.02 (8.4 – 11.63)	7.5 – 12.9	--	--	0.000
GIII	0 (0 – 2.81)	0 – 4.8	--	0.000	--
Test value	25.208				
P-value	<0.001 (HS)				

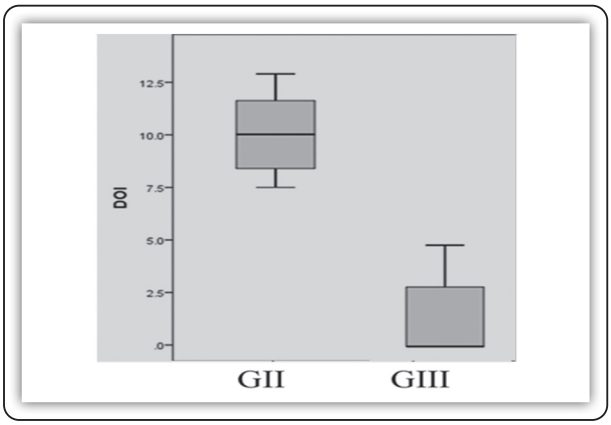

FIG (4) Bar fig representing tumor volume in the studied groups.

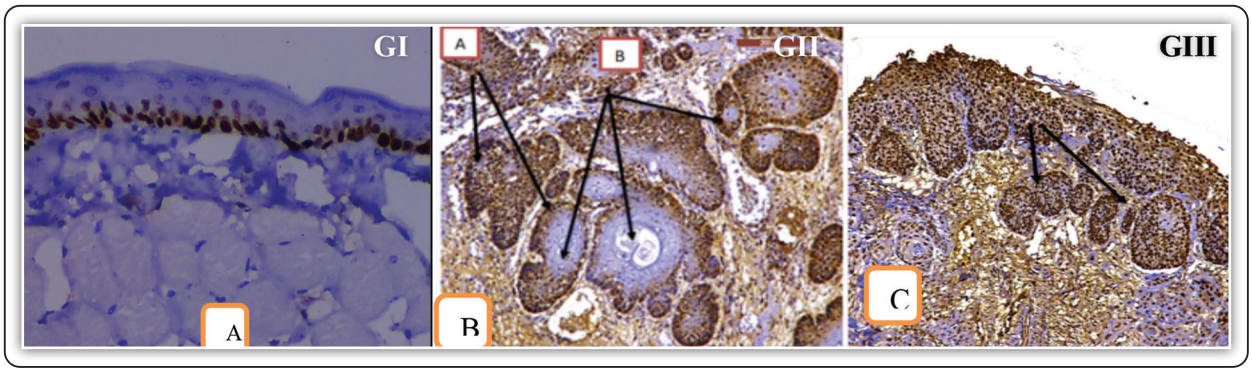

FIG (5) **(A)** Bmi1 IHC staining of GI showing positive nuclear expression limited to the basal and suprabasal epithelial layer (arrow) (Streptavidin biotin peroxidase, X 200); **(B)** Bmi-1 IHC staining of GII showing positive nuclear expression of the invading epithelial islands(arrows A) and negatively stained keratin pearl(arrows B) (Streptavidin biotin peroxidase, X 200); **(C)** Bmi-1 IHC staining of GIII showing positive nuclear expression throughout the epithelial nests, islands and invading tumor cells (arrows) (Streptavidin biotin peroxidase, X 200).

TABLE (3) Comparison between the studied groups regarding the mean area percentage of IHC stainability of cells with Bmi1 antibody.

	Bmi-1		Post Hoc analysis by LSD		
	Mean ± SD	Range	G I	G II	G III
G I	9.71 ±1.87	7.12 –12.8	--	0.000	0.000
G II	65.88 ±10.59	45.98 –77.02	0.000	--	0.000
G III	31.09 ±7.94	20.78 –44.98	0.000	0.000	--
Test value			**48.539**		
P-value			**<0.001 (HS)**		

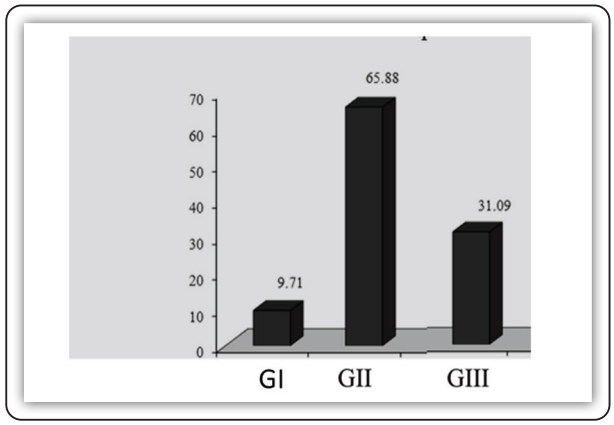

FIG (4) Chart showing the percentage of positive for Bmi-1 positive cells across all groups.

DISCUSSION

The morbidity and death rates for people with oral cancer remain relatively high despite simple access to the mouth cavity and major breakthroughs in therapy. The HBP is a valuable model for studying the biology, diagnosis, and therapy of oral carcinoma. The present study's GI histopathology findings are consistent with those of previous researchers[21-23] Positive nuclear expression of Bmi1 (9.71%) was seen by IHC of GI, however it was localized to the basal and supra-basal epithelial layers and was essentially undetectable in the other epithelial cell layers. This finding is consistent with what other researchers have found[18, 24]. According to Kalish et al. (2020) [24], Bmi1 is required for the self-renewal of both normal and CSCs.

After fourteen weeks of painting DMBA alone on the cheek pouches of hamsters, Balakrishnan et al. (2022) [25] observed 100% tumor development. Selvasundaram et al. (2018) [26]and Manimaran et al.(2017) [27] found similar outcomes. The ultimate carcinogenic metabolite of DMBA is dihydrodiol epoxide, which binds to and damages DNA, leading to mutation and carcinogenesis. This is due to the procarcinogenic character of DMBA, which is processed by phase I enzymes such cytochrome P450. Furthermore, ROS has been linked to all three phases of carcinogenesis, with evidence suggesting that ROS-mediated DNA damage can lead to structural modifications in DNA, the activation of proto-oncogenes, and the inactivation of tumor suppressor genes, all of which contribute to the neoplastic transformation that characterizes cancer[28].

GII compared to GI (p value= 0.001), showed a considerably higher mean area percentage of IHC staining of cells with Bmi1 antibody (65.88%), which was present in both the epithelial layers and invading tumor cells. Numerous investigations concur with this conclusion. In head and neck carcinomas, namely OSCC, Herzog et al. (2021)[29] demonstrated that Bmi1 was required for EMT throughout tumor growth. Overexpression of Bmi1 in tumor cells has been linked to stem-like characteristics and the production of the EMT, which has been linked to increased invasion, metastasis, and a poor prognosis[30]. Multiple tumor forms, including OSCC, showed strong evidence that Bmi1 was critical to invasive potential and promoted the maintenance and self-renewal of CSCs[29] Patel et al. (2018)[31] found that inhibiting Bmi1 might suppress CSC self-renewal and differentiation, as well as the malignant biological behavior of cancer. In addition to being linked to lymph node metastases and clinical stage, Bmi1 expression was associated with poor overall survival, as reported by Curtarelli et al. (2018) [17].

In the current study, the histopathological results of GIII showed that, 40% hamsters exhibited SCC with superficial invasion of malignant cells, It didn't go further into C.T. than the sub epithelium area, with the mean DOI (0–2.81) mm, while 20% hamster showed carcinoma in situ, 30% hamsters showed moderate epithelial dysplasia and 10% hamster showed mild epithelial dysplasia. This is findings in consistence with that shown by other researchers in different tumors Gunasekaran et al, (2017) [32] concluded that, Research using a mouse model of nitrosamine-induced carcinoma of the liver found that oral administration of piperine mediated lack of benzo pyrene metabolism through a direct contact with cytochrome P450 enzyme, hence eliminating cancer severit . While piperine was reported to stop the cell cycle at G0/G1 phase in human cancer of the prostate cell lines, research by Siddiqui et al. (2017)[12] showed that treatment of KB cell lines (human epithelial carcinoma cells) with 100 and 200 M piperine for 12 resulted in significant amounts of ROS synthesizing, which causes cell death by triggering the caspase-3 pathway in cancerous cells.

Positive nuclear expression was seen in all dysplastic and invading malignant cells when the Bmi1 antibody was used for IHC labeling of GIII, with a mean percentage of 31.09 and a very significant difference (p value 0.001) from GII. There have been various studies showing that piperine therapy down regulates CSCs, but to the best of our knowledge, this is the first research to examine therapeutic effectiveness of piperine on IHC staining utilizing Bmi1 as a one of CSCs.

Thao et al. (2021) [33] shown the effectiveness of piperine in limiting the formation of CSCs while being harmless to normal cells by creating nanoliposomal complexes of piperine and anti-CD133 monoclonal antibodies. The Wnt/ catenin pathway and nuclear localization of -catenin in colorectal cancer cell lines were both found to be blocked by piperine by Almeida et al. (2020) [34] Similarly, the combination of piperine and curcumin, which inhibits the Wnt/-catenin signaling pathway and, therefore, limits the creation of mammospheres, affects the self-renewal capacity of breast CSCs was shown to have a similar effect on these cells[35].

CONCLUSIONS

This study demonstrated that, piperine could inhibit HBP SCC formation and progression.

Bmi1 downregulation has an inverse proportion to increased degree of malignancy of HBP SCC, in addition to downregulation of Bmi1 can predict the therapeutic potential of piperine in OSCC.

REFERENCES

1. Boceila E, Atef A, Hassan M, Ali M, Khalele B, Shaban MJAiC, et al. Epidemiology of orofacial malignancies in Egypt (2016-2021): A reappraisal account. 2022;2(1): 24-36.
2. Wong T, Wiesenfeld D. Oral cancer. Australian dental journal. 2018;63:S91-S9.
3. Kerawala C, Roques T, Jeannon J, Bisase B. Oral cavity and lip cancer: United Kingdom national multidisciplinary guidelines. The Journal of Laryngology & Otology. 2016;130(S2):S83-S9.
4. Mohan M, Jagannathan N. Oral field cancerization: an update on current concepts. Oncology reviews. 2014;8(1).
5. Chen S-H, Hsiao S-Y, Chang K-Y, Chang J-Y. New insights into oral squamous cell carcinoma: From clinical aspects to molecular tumorigenesis. International Journal of Molecular Sciences. 2021;22(5):2252.
6. Ahmed SP, Jayan L, Dineshkumar T, Raman SJSJoRiDS. Oral squamous cell carcinoma under microscopic vision: A review of histological variants and its prognostic indicators. 2019;10(2):90.
7. Rajasekaran D, Kowsalya R, Selvasundaram R, Manoharan S. Enicostemma littorale protects cell surface abnormalities during DMBA-induced hamster buccal pouch carcinogenesis. Int J Pharma Bio Sci. 2015;6:104-9.
8. Peeters F, Van Dessel J, Croonenborghs TM, Smeets M, Sun Y, Willaert R, et al. Value of six comorbidity scales for predicting survival of patients with primary surgery for oral squamous cell carcinoma. 2022;44(5):1142-52.
9. Bauer A, Brönstrup MJNpr. Industrial natural product chemistry for drug discovery and development. 2014; 31(1):35-60.

10. Rasool Hassan BJPAA. Medicinal plants (importance and uses). 2012;3(10):2153-435.
11. Lagisetty P, Vilekar P, Sahoo K, Anant S, Awasthi V. CLEFMA-an anti-proliferative curcuminoid from structure-activity relationship studies on 3,5-bis(benzylidene)-4-piperidones. Bioorganic & medicinal chemistry. 2010;18(16):6109-20.
12. Siddiqui S, Ahamad MS, Jafri A, Afzal M, Arshad MJN, cancer. Piperine triggers apoptosis of human oral squamous carcinoma through cell cycle arrest and mitochondrial oxidative stress. 2017;69(5):791-9.
13. de Souza Grinevicius VMA, Kviecinski MR, Mota NSRS, Ourique F, Castro LSEPW, Andreguetti RR, et al. Piper nigrum ethanolic extract rich in piperamides causes ROS overproduction, oxidative damage in DNA leading to cell cycle arrest and apoptosis in cancer cells. 2016;189:139-47.
14. Hussein AM, El-Sheikh SM, Darwish ZE, Hussein KA, Gaafar AIJADJ. Effect of genistein and oxaliplatin on cancer stem cells in oral squamous cell carcinoma: an experimental study. 2018;43(1):117-23.
15. Al-Dosoki MA A-AA, Omar AMZ, Zouair MGA. Flow cytometric assessment of nivolumab and/or epigallocatechin-3-gallate on cancer stem cells of DMBA induced hamster buccal pouch carcinoma. Medical Science. 2021;25(118):3206-21.
16. Simple M, Suresh A, Das D, Kuriakose MAJOo. Cancer stem cells and field cancerization of oral squamous cell carcinoma. 2015;51(7):643-51.
17. Curtarelli RB, Gonçalves JM, Dos Santos LGP, Savi MG, Nör JE, Mezzomo LAM, et al. Expression of cancer stem cell biomarkers in human head and neck carcinomas: a systematic review. 2018;14(6):769-84.
18. Wu T-F, Li Y-C, Ma S-R, Bing-Liu, Zhang W-F, Sun Z-JJTB. Expression and associations of TRAF1, BMI-1, ALDH1, and Lin28B in oral squamous cell carcinoma. 2017;39(4):1010428317695930.
19. Gkoulioni V, Eleftheriadou A, Yiotakis I, Ferekidou E, Chrisovergis A, Lazaris AC, et al. The efficacy of imiquimod on dysplastic lesions of the oral mucosa: an experimental model. 2010;30(7):2891-6.
20. Wester A, Eyler JT, Swan JWJJcr. Topical imiquimod for the palliative treatment of recurrent oral squamous cell carcinoma. 2017;3(4):329-31.
21. Shamia AYM, Abd-Alhafez A-A, Al-qalshy ES, Zouair MGA. Therapeutic efficacy of time-dependent cetuximab on experimentally induced hamster buccal pouch carcinoma.
22. Martínez B DA, Barato Gómez PA, Iregui Castro CA, Rosas Pérez JEJBri. DMBA-induced oral carcinoma in Syrian hamster: Increased carcinogenic effect by dexamethasone coexposition. 2020;2020.
23. Ezzat SK, AbuElkhair MT, Mourad MI, Helal ME, Grawish MEJB, reports b. Effects of aqueous cinnamon extract on chemically-induced carcinoma of hamster cheek pouch mucosa. 2017;12:72-8.
24. Kalish JM, Tang X-H, Scognamiglio T, Zhang T, Gudas LJJCb, therapy. Doxycycline-induced exogenous Bmi-1 expression enhances tumor formation in a murine model of oral squamous cell carcinoma. 2020;21(5):400-11.
25. Balakrishnan V, Ganapathy S, Veerasamy V, Duraisamy R, Sathiavakoo VA, Krishnamoorthy V, et al. Anticancer and antioxidant profiling effects of Nerolidol against DMBA induced oral experimental carcinogenesis. 2022:e23029.
26. Selvasundaram R, Manoharan S, Buddhan R, Neelakandan M, Murali Naidu RJM, biochemistry c. Chemopreventive potential of esculetin in 7, 12-dimethylbenz (a) anthracene-induced hamster buccal pouch carcinogenesis. 2018;448(1):145-53.
27. Manimaran A, Buddhan R, Manoharan SJAJoT, Complementary, Medicines A. Emodin downregulates cell proliferation markers during DMBA induced oral carcinogenesis in golden Syrian hamsters. 2017;14(2):83-91.
28. Naveenkumar C, Raghunandhakumar S, Asokkumar S, Devaki T. Baicalein abrogates reactive oxygen species (ROS)-mediated mitochondrial dysfunction during experimental pulmonary carcinogenesis in vivo. Basic & clinical pharmacology & toxicology. 2013;112(4):270-81.
29. Herzog AE, Warner KA, Zhang Z, Bellile E, Bhagat MA, Castilho RM, et al. The IL-6R and Bmi-1 axis controls self-renewal and chemoresistance of head and neck cancer stem cells. 2021;12(11):1-12.
30. Chou C, Yang N, Liu T, Tai S, Hsu D-S, Chen YJCR. Chromosome Instability Modulated by BMI1-AURKA Signaling Drives Progression in Head and Neck Cancer (vol 73, pg 953, 2013). 2017;77(11):3125-6.
31. Patel N, Garikapati KR, Makani VKK, Nair AD, Vangara N, Bhadra U, et al. Regulating BMI1 expression via miRNAs promote Mesenchymal to Epithelial Transition (MET) and sensitizes breast cancer cell to chemotherapeutic drug. 2018;13(2):e0190245.
32. Gunasekaran V, Elangovan K, Devaraj SNJF, Toxicology C. Targeting hepatocellular carcinoma with piperine

by radical-mediated mitochondrial pathway of apoptosis: An in vitro and in vivo study. 2017;105:106-18.

33. Thao DT, Minh LN, Anh TTM, Thi Nga N, Hue PTK, Van Kiem PJNPC. The improved anticancer activities of piperine nanoliposome conjugated CD133 monoclonal antibody against NTERA-2 cancer stem cells. 2021;16(2):1934578X21998184.
34. de Almeida GC, Oliveira LF, Predes D, Fokoue HH, Kuster RM, Oliveira FL, et al. Piperine suppresses the Wnt/β-catenin pathway and has anti-cancer effects on colorectal cancer cells. 2020;10(1):1-12.
35. Kakarala M, Brenner DE, Korkaya H, Cheng C, Tazi K, Ginestier C, et al. Targeting breast stem cells with the cancer preventive compounds curcumin and piperine. Breast cancer research and treatment. 2010;122(3):777-85.